Journal of Environmental Radioactivity 164 (2016) 369–376

Contents lists available at ScienceDirect

Journal of Environmental Radioactivity

journal homepage: www.elsevier.com/locate/jenvrad

Application of banana peels nanosorbent for the removal of radioactive minerals from real mine water

Opeyemi A. Oyewo [a, *], Maurice S. Onyango [a], Christian Wolkersdorfer [b, c]

[a] Department of Chemical, Metallurgical and Materials Engineering, Tshwane University of Technology, Pretoria, 0001, South Africa
[b] SARChI Chair for Mine Water Management, Department of Environmental, Water, and Earth Sciences, Tshwane University of Technology, Pretoria, 0001, South Africa
[c] Lappeenranta University of Technology, Laboratory of Green Chemistry, Sammonkatu 12, 50130, Mikkeli, Finland

ARTICLE INFO

Article history:
Received 5 May 2016
Received in revised form
21 July 2016
Accepted 15 August 2016

Keywords:
Banana peel
Mechanical milling
Nanostructure
Adsorption
Actinides

ABSTRACT

Transformation of agricultural waste such as banana peels into a valuable sorbent material has been proven effective and efficient in wastewater treatment. Further, transformation into nanosorbent to enhance the removal capacity of actinides (uranium and thorium) from synthetic and real mine water is extensively investigated in this study. The nanosorbent samples before and after adsorption were characterised by X-ray diffraction (XRD), Fourier transform infra-red (FTIR), zetasizer nanoseries and scanning electron microscopy (SEM) while the amount of radioactive substances adsorbed was determined by inductively coupled plasma optical emission spectroscopy. Results revealed that there was a crystallite size and particle size reduction from 108 to 12 nm and <65,000 nm to <25 nm respectively as a function of milling time. Furthermore, appearance and disappearance of nanofibers via milling was noticed during structural analysis. The functional groups responsible for the banana peels capability to coordinate and remove metal ions were identified at absorption bands of 1730 cm^{-1} (carboxylic groups) and 889 cm^{-1} (amine groups) via FTIR analysis. Equilibrium isotherm results demonstrated that the adsorption process was endothermic for both uranium and thorium. The Langmuir maximum adsorption capacity was 27.1 mg g^{-1}, 34.13 mg g^{-1} for uranium and 45.5 mg g^{-1}, 10.10 mg g^{-1} for thorium in synthetic and real mine water, respectively. The results obtained indicate that nanostructured banana peels is a potential adsorbent for the removal of radioactive substances from aqueous solution and also from real mine water. However, the choice of this sorbent material for any application depends on the composition of the effluent to be treated.

1. Introduction

Radioactive contaminants were first discovered prior to World War II during a test carried out on mineral waters from the mines. The results indicated the presence of abnormally high concentrations of natural radioelements. This was because the newly discovered materials seemed to possess curative powers (Eisenbud and Gasell, 1997). Aside from the mines, radionuclides such as uranium (U) and thorium (Th) find their way into the environment and ground water through the nuclear, metallurgy and ceramic industries in which their usage is paramount. Thorium can also be used as a nuclear fuel through breeding to uranium-233 (U-233). In fact, major possibilities for U contamination to the ground water might be from industrial operation of extracting plutonium from irradiated U. It has been reported by Dutch research organisations that the rising demand for uranium to produce nuclear energy has led to an increase of uranium mining in several African countries (Sheree, 2011). Chantelle (2015) also reported that heavy rainfalls have resulted in the rapid rise of radioactive substances in underground water levels in Johannesburg, South Africa. The fact that radioactive substances such as U and Th are very toxic and highly harmful in small amounts, gives an additional reason for extensive investigation in the area of radioactive removal.

Even though U and Th are weakly radioactive and unstable, they are mostly in a constant state of decay, searching for more stable arrangement, they were still discovered to be present in municipal and drinking water (Organization, 2004). This has led some countries to require that the labels on bottled mineral waters should

* Corresponding author.
E-mail address: atiba.opeyemi@gmail.com (O.A. Oyewo).

http://dx.doi.org/10.1016/j.jenvrad.2016.08.014
0265-931X/

contain information on the measurement of radioactivity of the spring from which the water was obtained (Lewis, 1955). Lorenz (1944) reported the incidence of one multigenerational uranium miner in United Kingdom diagnosed with fatal lung diseases which later resulted to lung cancer. This was contacted through erosion by flowing U water in the mine environment. Therefore more research has to be done to develop technologies that can remove completely radioactive materials from mine water before it is discharged to the environment.

The techniques used to address this problem by several researchers have been largely inefficient and ineffective. For instance, techniques like coagulation, co-precipitation, filtration, ion exchange, membrane separation and adsorption (Rein, 2013) have been investigated for the treatment of radioactive laden water. Riodan et al. (1997) combined precipitation and biosorption methods using residual brewery yeast as biosorbent media and reported 360 mg/g biosorption capacity. This confirms the efficiency of these methods; however, they are not environmentally friendly due to the requirement of large settling tanks for the precipitation of voluminous alkaline sludge which requires subsequent treatment. Adsorption process is highly economical and capable of removing contaminants even at trace level. The use of this technique in water and wastewater treatment due its simplicity, low cost of operation and wide end use has been reported before (Naeem et al., 2007). However, the performance of any adsorption process is highly dependent on the choice of an appropriate media. Activated carbon is one of the common adsorbents that are highly efficient in uranium and thorium removal from aqueous solution and acidic medium, but it is highly expensive to develop (Ahmed et al., 2014; Loukiahadjittofi, 2012). Anirudhan et al. (2013) reported 2.4 mg/g adsorption capacity for thorium removal onto carboxylate-functionalized graft co-polymer derived from titanium dioxide-densified cellulose. This is considered an inefficient and non-effective adsorbent due to its lower capacity compared to natural materials with high content of cellulose. For instance, pineapple peels, sugarcane bagasse, coconut coir, citrus limetta peels (Hossain et al., 2012; Sachin and Sanjeev, 2014) and banana peels nanosorbent (used in this study) are cellulose constituent materials. The major structural components of banana peels are cellulose (75%) and nanofibers (5.1%). Cellulose is a glucose polymer bounded in the β-1,4 linkage configuration (Riantong et al., 2013; Franceiele et al., 2014).

Even though banana peels have been used earlier as a base material for the development of many adsorbents to remove metal ions, low adsorptive performance was reported (Bakiya and Sudha, 2012; Ashok et al., 2010). It is speculated that the effect of some properties such as surface area and particle size in material preparation could be responsible for this low performances. For instance, Castro et al. (2011) reported the use of banana peels (particle size 35–45 μm) with adsorption capacity of 20 mg/g for copper removal from aqueous solution. This implies that the performance would have been more efficient with increment of active sites. It was reported that advances in nanoscience and nanotechnology have expanded the ability to develop nanomaterials with enhanced properties to solve the current problems in water treatment. As a result of their small size, nanomaterials can exhibit an array of unique novel properties which can be utilized in the development of new metal treatment technologies and improvement of existing ones (Arup and Jayanta, 2015).

In this study, banana peels were transformed into nano size in order to take advantage of their improved chemical and physical properties for mine water treatment. Nanostructure formation was confirmed through characterization and radioactive substances removal performance explored in a batch adsorption mode. Adsorption isotherm results were interpreted using Langmuir and Freundlich isotherms.

2. Experimental

Banana peels (*Musa paradisiacal*) were simply separated from bananas and cut into smaller pieces while still wet. The peels were washed with deionized water to remove the adhering dirt and then sun dried for 10 days. The dried peels were crushed and screened to obtain a particle size of <65 μm. Acidic and alkali treatment was then done to enhance their sorption capacity using NaOH and HNO_3. These chemicals were obtained from Sigma Aldrich, South Africa and were of analytical grade.

Mechanical milling of crushed banana peels (<65 μm) was carried out in a planetary continuous ball mill machine (PM 100 CM) at a constant speed of 200 rpm using 10:1 powder to ball ratio. The energy consumption of the milling process was determined to be 1.5 kJ/h. The wet milling was done for 30 h and the samples were taken at 10 h intervals to observe the structural changes. Ethanol was used as a process control agent as well as a bleaching agent to remove the yellowish colour of ripe banana peels. The microstructural characterization of milled banana peels was carried out with a wide angle diffractometer using analytical empyrean advance diffractometer with a quartz sample holder, with Cu K α radiation (λ = 0.15,406 nm, 40 kV, 40 mA and increment 0.01°). The high score plus program was used to determine the crystalline sizes at different milling times (0 h–30 h), using the PROFILE-FIT package (Mhadhbi et al., 2010). Moreover, the physical profiles such as width broadening of the peaks were calculated from the integral width of the physical broadening profile by the Scherrer equation:

$$\tau = \frac{K\lambda}{\beta\ COS\ \theta} \quad (1)$$

where τ is the mean size of the ordered (crystalline) domains, which may be smaller or equal to the grain size; K is a dimensionless shape factor with a value close to unity; λ is the X-ray wavelength; and β is the line broadening at half the maximum intensity (FWHM) after subtracting the instrumental line broadening in radians and θ is the bragg angle.

The Fourier transform infrared spectroscopy (FTIR) analysis was done to identify the functional groups using a Perkin Elmer Spectrum 100 spectrometer. The spectra were recorded in the 500–4000 cm^{-1} range at a resolution of 4 $cm^{-1.}$ The morphology and composition of the milled samples were characterized by SEM/EDX using a JEOL JSM-7600F Field Emission Scanning Emission Microscope (FESEM), running at an accelerating voltage of 2 kV. The adsorbent zeta potential analysis was done using zetasizer nanoseries (Malvern instruments). Synthetic water was prepared in binary solution using uranium and thorium nitrate salts. Real mine tailing seepage was obtained from one of the gold mining operations in South Africa situated at about 40 km South-West of Gauteng province. Batch equilibrium experiments were performed to determine the adsorptive performance of banana peels nanosorbent (BPN) on the removal of radioactive substances from aqueous solution. Firstly, the effect of solution pH was studied in order to determine the optimum pH for the process. Using either NaOH (0.1 M) or HCl (0.1 M), the initial pH was adjusted from 2 to 10 (the equilibrium pH is presented in Table 3). In addition, 0.1 g of BPN was added to 100 mL plastic bottles containing 50 mL solution of actinides (radioactive) in synthetic and real mine water. U and Th of similar initial concentrations (100 mg/L) were employed in synthetic water in binary solution. The real mine water contained 55.8 mg/L and 18.8 mg/L of U and Th, respectively. Thereafter, the bottles were placed in a thermostatic shaker operated at 200 rpm for 24 h. At the end of the contact period, the samples were filtered

using syringe filter of 0.45 μm pore size and the filtrate was analysed by inductive coupled plasma optical emission spectroscopy (ICP-OES) to determine the residual concentration of actinides (U and Th). The above procedure was repeated to determine the effect of sorbent mass, initial concentration and temperature on the amount of actinides adsorbed. The effect of sorbent loading was explored by varying the mass of the sorbent from 0.01 g to 0.3 g, while the effect of concentration was explored by varying the concentration of the actinides synthetic solution from 20 mg/L to 200 mg/L. These concentrations are within the solubility range of Th in water (Alexander et al., 1973; Fawwaz and Ghadeer, 2015) by the decomposition of thorium nitrate salt at room temperature. Even though the South Africa guideline values as set by the Department of Water Affairs and Forestry require a concentrations of less 70 μg/l Uranium in wastewater discharge (Botha et al., 2009); higher concentrations were selected for this study in order to test the performance of the material. Some previous studies such as Firas (2013) have used up to 1000 mg/L U and Th solutions. However, for the real mine water, the concentration was not changed except for the isotherm investigation. Finally, the effect of temperature was studied by varying the temperature from 25 °C to 45 °C. The sorbent mass was fixed at 0.2 g as the concentration was varied in synthetic and real mine water for isotherm investigation.

The percentage removal efficiency R_t was calculated (Equation (2)) as well as the equilibrium uptake q_e (mg/g), Equation (3):

$$R_t = \frac{C_o - C_e}{C_o} \cdot 100 \tag{2}$$

$$q_e = \frac{C_o - C_e}{m} \cdot V \tag{3}$$

where C_0 (mg/L) is the initial actinides concentration, C_e (mg/L) the concentration of actinides at equilibrium, V is the volume of the sample (L) and m the mass of adsorbent (g).

Meanwhile, equilibrium isotherm data were interpreted using the Langmuir and Freundlich models. The linear forms of the Langmuir (Equation (4)) and Freundlich (Equation (5)) adsorption isotherms equations are given by:

$$\frac{C_e}{q_e} = \frac{1}{q_o b} + \frac{C_e}{q_o} \tag{4}$$

$$\log q_e = \log K_F + \frac{1}{n} \log C_e \tag{5}$$

where b is the Langmuir constant, q_o is the Langmuir maximum adsorption capacity, K_F and n are the Freundlich parameters related to adsorption capacity and adsorption intensity, respectively.

3. Results and discussion

3.1. Characterization of adsorbent

3.1.1. Fourier transform infra-red (FT-IR) spectroscopy

The FT-IR spectra of crushed banana peels powder (unmilled), and at the following milling times: 10 h, 20 h, 30 h together with the used (30 h milled) BPN are shown in Fig. 1. The bands at 3486–3286 cm^{-1} are due to O–H stretching while the C–H stretching is identified at 2920–2951 cm^{-1}. The band at 1730 cm^{-1} is attributed to the C=O bond of carboxylic acid (Castro et al., 2011). The wavelength of this band becomes lower as the milling progresses suggesting that this phase might be sensitive to mechanical stress. The band at 889 cm^{-1} is attributed to an amine group and as can be seen, this band disappears in the after-use BPN media

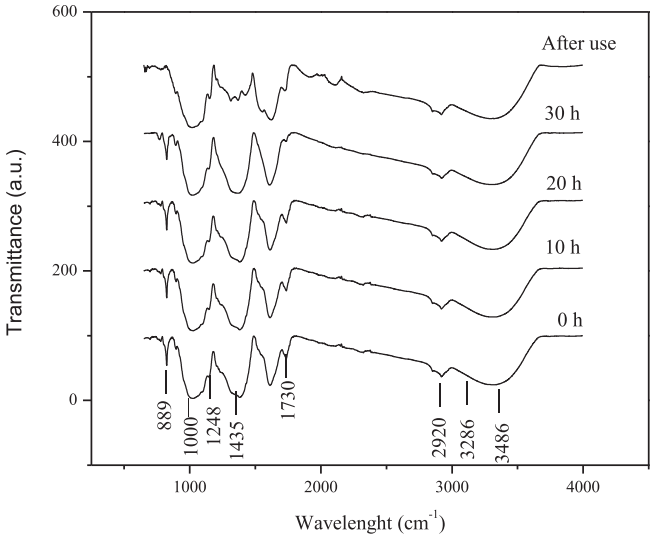

Fig. 1. FT-IR Spectra of banana peels at different milling times and after actinides (U and Th in binary solution) adsorption onto BPN.

indicating that the amine group is majorly responsible for the removal of radioactive substances (Spiro et al., 2016). A clear band was observed at 2000 cm^{-1} (in the after use media), indicating a chemical interaction between radionuclide and banana peels nanosorbent.

3.1.2. Scanning electron microscopy (SEM) analysis

This analysis revealed information about the morphology of the banana peels powders at different milling times and after adsorption (Fig. 2). The crushed powder particles were found to be nearly equiaxed (Fig. 2a) with an average size of 65 μm. The fracture of these particles can be seen in Fig. 2(b) (10 h) which brought an onset appearance of fibres within the particles and the shape of the particles became more regular and flattened, still equiaxed with considerable change in the particle size. The disappearance of fibres due to further decrease in particle size by fracturing during the milling process was observed indicating the nanostructure of the fibre and particle formation in 20 h milled powder Fig. 2 (c); it is also observed that the particles were regularly and uniformly shaped. Moreover, further milling leads to a matrix of randomly welded thin layers of highly deformed particles (Mhadhbi et al., 2010). Probably some un-deformed fragments of the initial powder particles are embedded as seen in Fig. 2(d) (30 h). Agglomeration of the particles due to cold welding was observed in 30 h milled powder and seen as clusters of the particles on the surface of the material. This suggests that the rate of welding is higher than the rate of fracturing of the particles at this stage Fig. 2(d). Fig. 2 (e) shows banana peels nanosorbent after-adsorption form which brought the re-appearance of nanofibers on the surface of the material. This shows that the earlier disappearances of the nanofibers were not permanent but invisible due to their nano size and cold welding. Generally, it can be clearly observed that the particles size reduction as a result of mechanical milling was increasing continuously up to 20 h of milling and also the onset regularity of the shape was noticed. A slight decrease was observed above 20 h due to cold welding of the small particles to the surface of big particles which bring forth agglomeration, suggesting discontinuation of the milling process.

3.1.3. X-ray diffraction (XRD) analysis

X-ray diffraction (XRD) analysis results of the banana peels

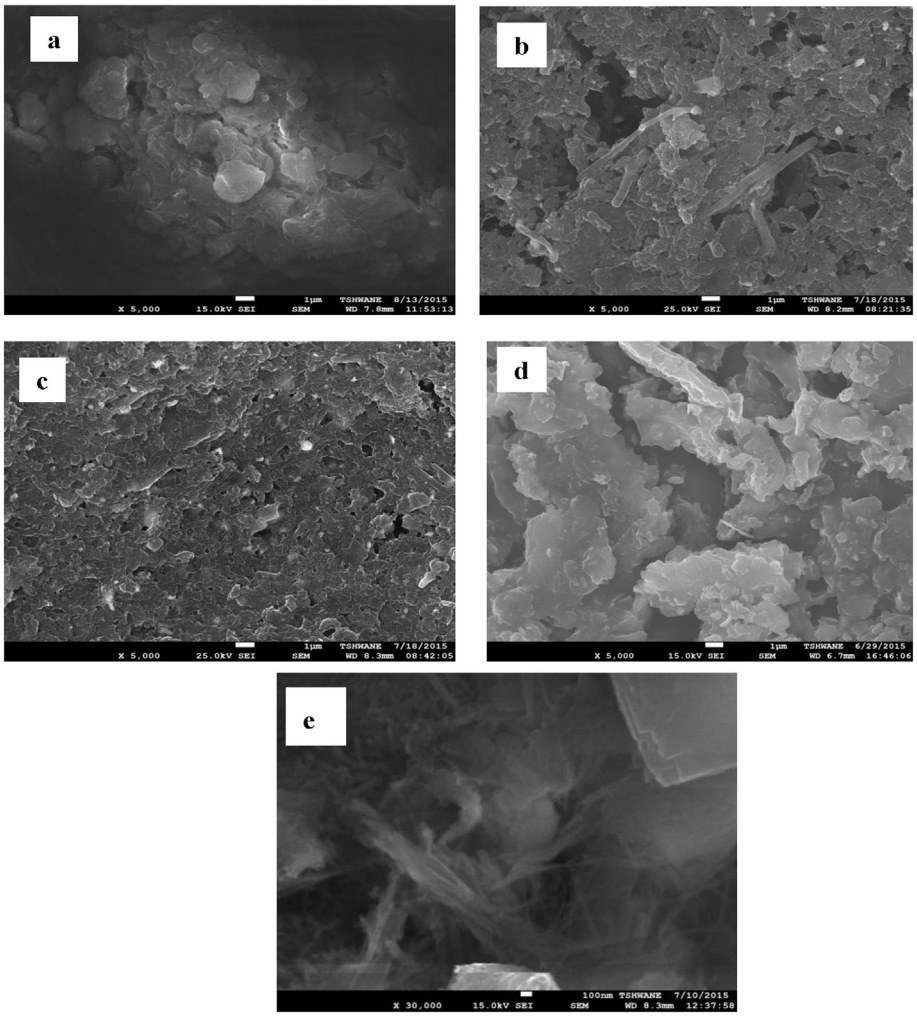

Fig. 2. SEM images of the banana peels powder particles mechanically alloyed: (a) crushed, (b) 10 h milled sample(c) 20 h milled sample (d) 30 h milled sample (e) 30 h after-use form.

before, after different milling times and after adsorption form are shown in Fig. 3. Prior to milling, banana peels displayed an amorphous character with a certain degree of crystallinity which can be seen as a bump at a 2θ angle 10°–50°. Within the same range, very clear peaks are observed at 2θ angles of 20° and 23°; the latter is also present after milling but with reduced intensity (Suryanarayana, 2001). This suggests reduction in the amount of corresponding phase ($C_{84}H_{72}N_{16}O_{16}$), and this phase re-appeared with higher intensity after adsorption indicating the chemical reaction between this phase and radioactive contaminants. The bump (amorphous) disappeared as the milling proceeded, indicating that the material becomes purely crystalline due to its nanostructure (Heguang et al., 2015). Additionally, the increase in broadening and intensity of the peaks with milling time can be clearly seen, and this is an indication of a decrease in crystallite size as the milling progresses (Bushroa et al., 2012). A number of phases are identified in banana peels nanosorbent and the prominent peaks correspond to amine and carboxylic groups which are the main groups responsible for its ability to remove metal ions (Hossain et al., 2012). The appearance of new peaks in the milled samples such as $C_4H_4O_8$ indicates the formation of new phases as a result of continuous milling and ethanol used as a process control for wet milling. The reduction in intensity and disappearance of some prominent peaks such as ($C_{12}H_{28}N_4O_{12}$), ($C_2H_{16}N_4$), ($C_{84}H_{72}N_{16}O_{16}$), ($C_{52}H_{92}O_4$) and (Ca_2) respectively was observed in after adsorption BPN sample indicating the contributions of these phases in actinides removal

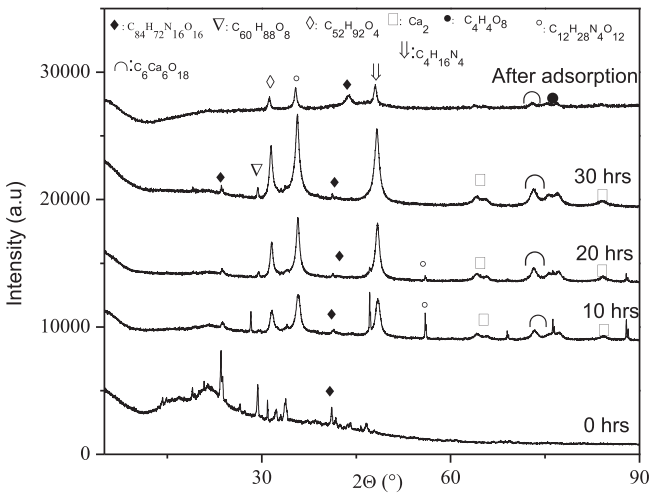

Fig. 3. X-ray diffraction patterns of crushed, mechanically milled samples as a function of the milling time (0 h, 10 h, 20 h and 30 h), and after-adsorption samples.

from synthetic and real mine water.

The crystallite size decreased from 108 nm to 12 nm as milling time increases due to continuous broadening/widening of the peaks as the milling progressed (Fig. 3) (Venkateswarlu et al., 2014). Increase in milling time (0 h–10 h) results in a decrease in particle size from <65,000 nm to around <300 nm, and from <300 nm to <65 nm after 20 h and finally from <65 to <25 nm after 30 h milling time (Table 1). This confirms nanostructure (0–100 nm) formation.

3.1.4. Mine water characterization

The mine water used was found to contain other metal ions such as K, Ca, V, Cr, Fe and Mn as shown in Table 2. It was observed that some of these metal ions were also removed by adsorption on BPN, mostly the metal ion in similar categories with actinide such as transition metals (V and Mn).

3.2. Adsorptive performance of banana peels nanosorbent (BPN)

3.2.1. Effect of solution pH

Effect of solution pH on actinides removal (U and Th) from binary synthetic solution onto BPN together with the zeta potential of banana peels nanosorbent (BPN), and the real mine water onto BPN is shown in Fig. 4 and Fig. 5, respectively. A gradual increase in the radioactive uptake was observed with an increase in pH for synthetic water and mine water, respectively. However, a clear relationship between U and BPN was observed at pH 8 indicating the association between U and BPN potential at this pH. The chemistry of U and Th in aqueous solution especially in acidic medium is governed by the dioxo cation UO_2^{2+} and $[Th(H_2O)_9]^{4+}$ respectively (Langmuir, 1978); structural analogs of these species are known from the actinides such as PuO_2^{2+} and AmO_2^{3+}, thorium occurs exclusively as the tetra positive aqua ion in the solution. Krestou and Panias (2004) reported that between pH 2–3, Uranyl cations (UO_2^{2+}) are the only existing uranium (VI) bearing species in the solution. As the U concentration increases, the pH region where UO_2^{2+} prevails is shrunk, and as the pH increases especially from pH 6 upward, U and Th in the solution changes from positively charged species to negatively charged species (Yuehe et al., 1994). The neutral aqueous species $UO_2(OH)_2$ and $[Th(OH)2]^{2+}$ prevails in this region (pH 7–pH 10) under very low total U and Th at any ionic strength indicating that the higher removal observed in alkaline medium was due to precipitation of these species exist only in this pH region. It is possible that both adsorption and precipitation mechanisms were involved (Nwe nwe et al., 2008). Furthermore, non-solid experiment was done using 200 mg/L concentration of Th at room temperature and the results revealed that at pH 2: 200 mg/L, pH 4: 195.6 mg/L, pH 6: 110.1 mg/L, pH 8: 61.2 mg/L and pH 10:43 mg/L was recorded. This is indicating that the precipitation of Th started from pH 5 and increased with increase in pH till pH 10. Moreover, it was reported (Weijuan and Zuyi, 2002; Humelnicu et al., 2006; Talip et al., 2009) that the hydrolysis products and precipitation at pH > 4 must play an important role in the sorption of Th, low soluble mononuclear and polynuclear-polymeric hydrolysis products of a general type of thorium is formed at pH > 4.5. This is in line with observation in this study, since the optimum pH used was pH 4, negligible precipitation was observed.

Moreover, the higher concentration of Iron ox-hydrate (Fe (III)

Table 1
Summary of TEM and XRD analyses results of milled banana peel.

Milling time h	Average particle size (nm)	Mean crystallite size (nm)	Lattice strain (%)
0	<65,000	108	0.24433
10	<300	71	0.626
20	<65	20	0.64277
30	<25	12	0.69144

Table 2
Real mine water characterization before and after adsorption onto BPN results.

Elements	Initial Conc.(μg/L)	Final Conc.(μg/L)
U	58,800	8990
Th	18,800	36.2
K	230	112
Ca	459,233	33,713
V	112	46
Cr	5356	3417
Fe	7,151,533	6,596,314
Mn	89,057	5602

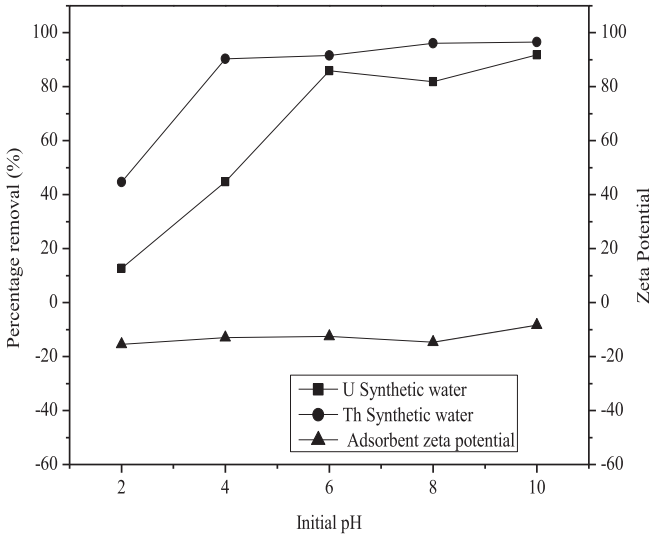

Fig. 4. Effect of solution pH in the adsorption of actinides in synthetic water onto banana peels nanosorbent (BPN) and zeta potential of BPN (Temp. 25 °C, duration 24 h, initial conc., 100 mg L^{-1} and sorbent mass 0.1 g).

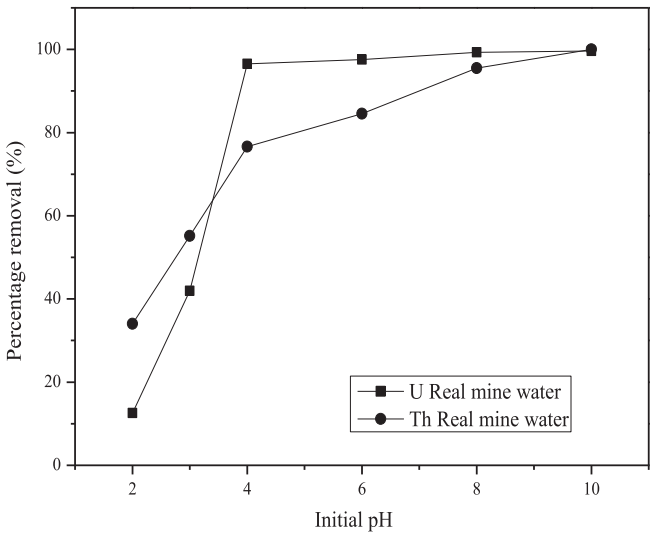

Fig. 5. Effect of solution pH in actinides real water onto banana peels nanosorbent (BPN)(Temp. 25 °C, duration 24 h, initial conc., U is 58.8 mg L^{-1}, Th is 18.8 and sorbent mass 0.1 g).

Table 3
Initial and equilibrium solution pH results in synthetic and real mine water.

Sample treated	pH before adsorption	Equilibrium pH(Synthetic)	Equilibrium pH(Real mine)
pH2	2.10	2.19	2.30
pH3	3.10	–	3.29
pH4	4.10	4.37	4.40
pH6	6.10	6.19	6.70
pH8	8.20	8.32	8.48
pH10	10.1	10.42	11.10

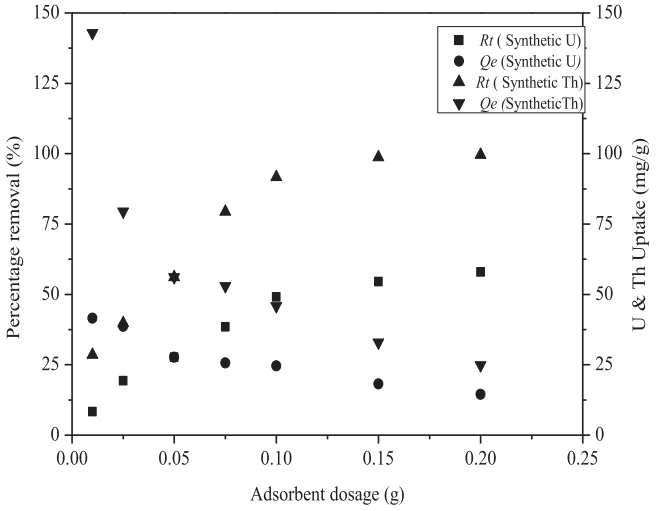

Fig. 6. Effect of adsorbent dosage on actinides adsorption (synthetic water; initial conc. 100 mg L^{-1}, and pH 4.10, Temp. 25 °C, duration 24 h).

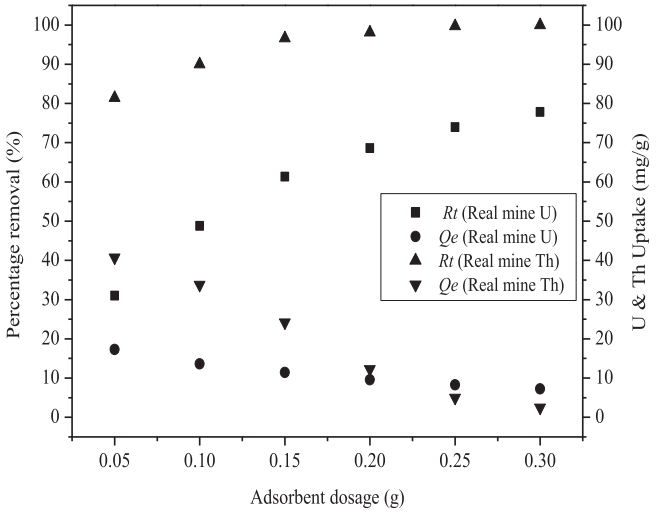

Fig. 7. Effect of adsorbent dosage on actinides adsorption (real mine water; initial conc. U 58.8 mg L^{-1}, Th 18.8 mg L^{-1} and pH 3.10, Temp. 25 °C, duration 24 h).

about 7151.5 mg/L) in real mine water (Table 2), instigated the precipitation of the solution at pH 3.5 which was earlier than the synthetic water. Therefore, the optimum pH for real mine water was considered pH 3.0 (Fig. 5) and was used for the subsequent studies. According to Margarete et al. (2004), the percentage relative amount of UO_2^{2+} and $[Th(H_2O)_9]^{4+}$ at pH 4 is about 80% and based on the chemistry of these ions discussed above, the optimum

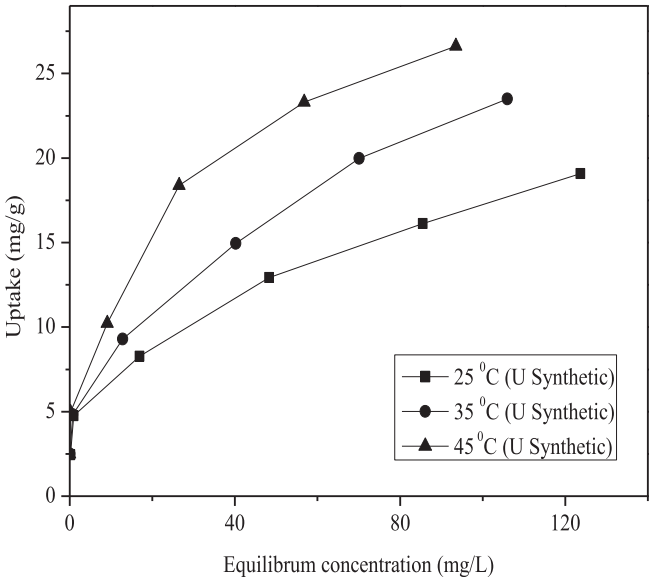

Fig. 8. Isotherms for uranium synthetic water sorption onto BPN (pH 4.10, Temp. 25–45 °C, duration 24 h, 20 mg/L to 200 mg/L, dosage 0.2 g).

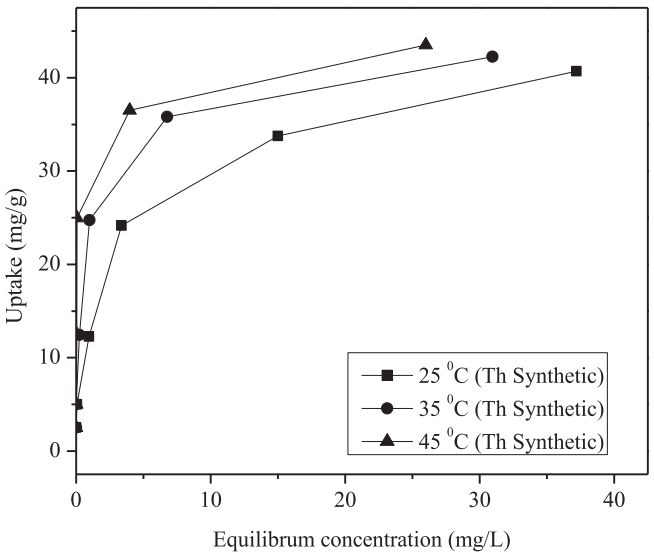

Fig. 9. Isotherms for thorium synthetic water sorption onto BPN (pH 4.10, Temp. 25–45 °C, duration 24 h, 20 mg/L to 200 mg/L, dosage 0.2 g).

pH used for the subsequent synthetic experiment was pH 4.1 (Fig. 4). In addition, the equilibrium pH in synthetic and real mine water was found to be 4.37 and 3.29 respectively. The increase in pH at equilibrium might be due to the protonation of radionuclide ions in the synthetic and mine water solution which caused the removal of hydrogen ions (Table 3).

3.2.2. *Effect of sorbent mass*

Figs. 6 and 7 show the effect of varying adsorbent dosage on the actinides synthetic and real mine water uptake efficiency. It can be seen that the percentage removal of actinides increases with an increase in the adsorbent dosage in synthetic and real mine water (Matteo et al., 2003; Margarete et al., 2004). This is because active sites available for actinides sorption are proportional to the adsorbent mass. Overall uptake efficiencies achieved in actinides sorption onto BPN in this study are higher compared with

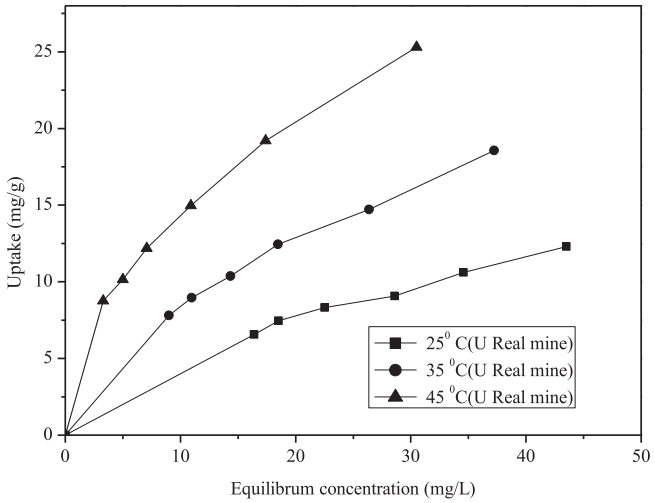

Fig. 10. Isotherms for uranium real mine water sorption onto BPN (real mine water; pH 3.10, Temp. 25 °C, duration 24 h).

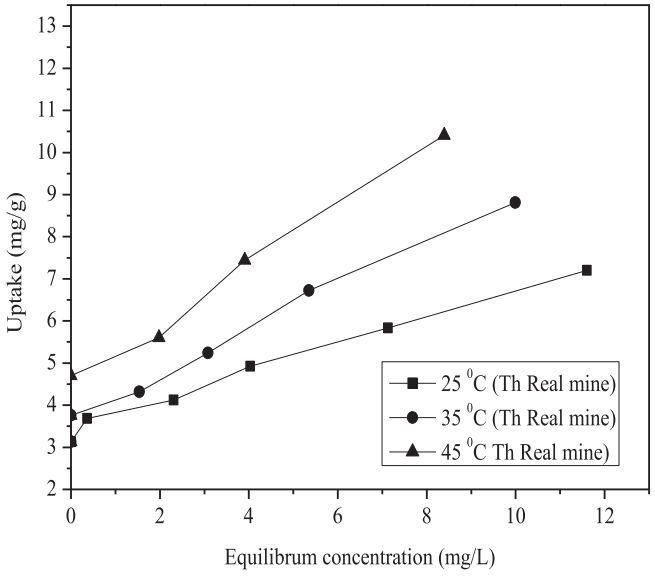

Fig. 11. Isotherms for thorium real mine water sorption onto BPN (real mine water; pH 3.10, Temp. 25 °C, duration 24 h).

radioactive uptake efficiency elsewhere (Anirudhan et al., 2013), especially for thorium.

Table 5
Isotherms parameters for uranium in synthetic and mine water adsorption onto BPN.

Temperature (°C)	Synthetic water			Mine water		
	Langmuir isotherm parameters					
	q_m (mg/g)	b (L/mg)	R^2	q_m (mg/g)	b (L/mg)	R^2
25	20	11.711	0.96	24.1	43.49	0.968
35	25	10.550	0.96	32.6	29.7	0.9814
45	27	6.912	0.97	34.13	12.04	0.973
	Freundlich isotherm parameters					
	K_F (L/g)	$1/n$	R^2	K_F (L/g)	$1/n$	R^2
25	2.583	0.443	0.998	1.23	0.61	0.998
35	2.945	0.412	0.999	2.11	0.60	0.999
45	6.999	0.30	0.998	4.76	0.49	0.998

3.3. Sorption isotherms

Temperature dependence of actinides sorption was explored by varying the temperature in the range of 25–45 °C. Figs. 8–10, 11 show sorption isotherms for synthetic U, Th and real mine U and Th onto BPN, respectively. It is observed that an increase in equilibrium concentration results in an increase in actinides equilibrium uptake in synthetic water. Also, an increase in adsorbent dosage increases the radioactive equilibrium uptake in real mine water. Moreover, the adsorption capacity increased with an increase in temperature in both cases, indicating that actinides sorption on BPN is a temperature dependent process. The enhanced sorption at higher temperatures may occur due to a decrease in the thickness of the interface surrounding the banana peels nanosorbent. There is also a possibility of an increase in the movement of the molecules with a rise in temperature; however, within the range of temperatures investigated in this study, this will not significantly affect the binding capacity of the adsorbent. The data provided from sorption equilibrium are used to describe the interaction between adsorbate and adsorbent for effective design of an adsorption process. Furthermore, sorption equilibrium data are used in comparing the performance of different media for a given sorption process. Consequently, the experimental data were analysed using Langmuir and Freundlich models. The Langmuir isotherm parameters q_o, which measures the monolayer capacity of the adsorbent and the predicted K_F values from the Freundlich isotherm increase as the temperature increases while the Langmuir constant b decreases with an increase in temperature in both cases. Since K_F is related to the sorption capacity, the observation matches the results presented in Figs. 8–10, 11, which show that sorption is enhanced at higher temperatures. Comparing the Langmuir and Freundlich adsorption isotherm correlation values (R^2), the

Table 4
Isotherms parameters for thorium in synthetic and mine water adsorption onto BPN.

Temperature (°C)	Synthetic water			Mine water		
	Langmuir isotherm parameters					
	q_m (mg/g)	b (L/mg)	R^2	q_m (mg/g)	B (L/mg)	R^2
25	41.7	1.55	0.992	7.22	9.5×10^{-1}	0.956
35	43.5	0.50	0.999	8.81	8.9×10^{-1}	0.94
45	45.5	0.20	0.999	10.10	4.6×10^{-1}	0.944
	Freundlich isotherm parameters					
	K_F (L/g)	$1/n$	R^2	K_F (L/g)	$1/n$	R^2
25	18.57	0.22	0.999	3.074	0.34	0.995
35	29.08	0.11	1	3.544	0.39	0.998
45	32.09	0.09	1	4.1712	0.43	0.999

Langmuir and Freundlich isotherms gave a good description of the thorium removal while uranium removal is described by the Freundlich isotherm only (see Tables 4 and 5).

4. Conclusion

Generally, it was concluded from this study that increased in surface area and particle size reduction improves banana peels sorbing capacity on radioactive removal from synthetic and real mine water. The crystallinity and phase changes in banana peel via mechanical milling were investigated and the crystallite size was found to decrease from 108 nm to 12 nm. The functional groups responsible for the removal of radioactive substances were found to be amine and carboxylic groups. The extent of adsorption was found to be controlled primarily by pH and temperature. Solution pH 4.10 and pH 3.0 were found to be favourable for the sorption of radioactive from synthetic and South African mine water, respectively. This is consistent with the chemical interaction between the hydrophilic surface of BPN and the strongly cationic radioactive species in acidic medium. It was also observed that a dosage in the range of 0.01–0.3 g of BPN was required for 99.99% removal of Th from 100 mg/L, 18.8 mg/L initial concentration and 70% removal of U from initial concentration of 100 mg/L, 58.8 mg/L both at pH 4.10, 3.0 from synthetic and real mine water, respectively. The BPN-Th and U interactions were found to be endothermic in nature due to higher uptake efficiency as temperature increases. The adsorption equilibrium was well described by both Langmuir and Freundlich adsorption isotherm for Th, and U was well described by Freundlich adsorption isotherm only. Given the low cost of natural sorbent media (BPN) and the competitive sorption capacity achieved through milling, this material can be considered as a potential candidate for treatment of radioactive contaminated water. On this note, transformations of other agricultural waste are highly recommended for further investigations.

Acknowledgements

The authors wish to appreciate national refund foundation (NRF) for funding grant number 94156, Dr Modiu O. Durowoju, Dr Saliou Diouf and Mr Fatoba O.S for their assistance in characterization and also for our fruitful discussions.

References

Ahmed, B., Rachid, R., Hocine, H., Sihem, K., Mohamed, B., 2014. The removal of uranium(VI) from aqeous solutions onto activated carbon developed from grinded used tire. Environ. Sci. Pollut. Res. 21, 684–694.
Anirudhan, T.S., Sreekumari, S.S., Jalajamony, S., 2013. An investigation into the adsorption of thorium(IV) from aqueous solutions by a carboxylate-functionalised graft copolymer derived from titanium dioxide-densified cellulose. J. Environ. Radioact. 116, 141–147.
Alexander, A., David, A., Ayala, S., 1973. Properties of aqueous thorium nitrate solutions. Part 1.—Densities, viscosities, conductivities, pH, solubility and activities at freezing point. J. Chem. Soc. 69, 1618–1623.
Arup, R., Jayanta, B., 2015. Nanotechnology in Industrial Wastewater Treatment, 12 Caxton Street. IWA Publishing, London.
Ashok, B., Bhagyashree, J., Ameeta, R.K., Smita, Z., 2010. Banana peel extract mediated novel route for the synthesis of silver nanoparticles. J. Colloids Surf. 368, 58–63.
Bakiya, L.K., Sudha, P.N., 2012. Adsorption of Copper (II) ion onto chitosan/sisal/banana fiber hybrid composite. J. Environ. Sci. 3, 453.
Botha, M., Bester, L., Hardwick, E., 2009. Removal of uranium from mine water using ion exchange at driefontein mine. In: International Mine Water Conference 19th – 23rd October 2009. WHO, Pretoria, South Africa.
Bushroa, A.R., Rahbari, R.G., Masjuki, H.H., Muhamad, M.R., 2012. Approximation of crystallite size and microstrain via XRD line broadening analysis in TiSiN thin films. Vacuum 86, 1107–1112.
Castro, R.S.D., Caetano, L., Ferreira, G., Padilha, P.M., Saeki, M.J., Zara, L.F., Martines, M.A.U., Castro, G.R., 2011. Banana peel applied to the solid phase extraction of copper and lead from river water: preconcentration of metal ions with a fruit waste. Ind. Eng. Chem. Res. 50, 3446–3451.
Chantelle, K., 2015. A Review of the Uranium Mining Industry in Africa Creamer Media. Creamer Media Mining Weekly.
Eisenbud, M., Gasell, T., 1997. Environmental Radioactivity:From Natural, Industrial and Military Sources, California.
Fawwaz, K., Ghadeer, A., 2015. Adsorption of uranium(VI) and thorium(IV) by insolubilized humic acid from Ajloun soil e Jordan. J. Environ. Radioact. 146.
Firas, S.A., 2013. Thorium removal from waste water using Banana peel and employment of Waste Residue. Adv. Nat. Appl. Sci. 3, 336–344.
Franceiele, M.P., Paulo, J., Florencia, C.M., 2014. Isolation and characterization of cellulose nanofibers from banana peels. Cellulose 21, 417–432.
Heguang, L., Tiehu, L., Tingting, H., Xing, Z., 2015. Effect of multi-walled carbon nanotube additiveon the microstructure and properties of pitch-derived carbon foams. J. Mater. Sci. 50, 7583–7590.
Hossain, M.A., Ngo, H.H., Guo, W.S., Nguyen, T.V., 2012. Biosorption of Cu(II) from water by Banana peel based biosorbent: experiments and models of adsorption and desorption. JWS 1, 87–104.
Humelnicu, D., Drochioiu, G., Sturza, M.I., Cecal, A., Popa, K., 2006. Kinetic and thermodynamic aspects of U(VI) and Th(IV) sorption on a zeolitic volcanic tuff. J. Radioanal. Nucl. Chem. 270, 637–640.
Krestou, A., Panias, D., 2004. Uranium (VI) speciation diagrams in the UO22+/CO32-/H2O system at 25oC. EJMP EP 4, 113–129.
Langmuir, D., 1978. Uranium solution mineral equilibrum at low temperatures with applications to sedimentary ore deposits. Geochimica Cosmochim. Acta 42 (6).
Lewis, W.L., 1955. Arthritis and Radioactivity. Christopher Publ. House, Boston.
Lorenz, E., 1944. Radioactivity and lung cancer; A critical review in miners of Schnerberg and Joachimstah. J. Natal. Cancer Inst. 5 (1).
Loukiahadjittofi, I.P., 2012. Thorium Removal from Acidic Aqueous Solutions by Activated Biochar Derived from Cactus Fibres Nicosia. University of Cyprus, Cyprus.
Matteo, C., Francesca, G., Mirko, D., Luigi, B., Mario, M., 2003. Adsorption of uranium, cesium and strontium onto coconut shell activated carbon. Radioanal. Nucl. Chem. 297, 9–18.
Margarete, K., Wheelerb, W.N., Meinrathc, G., 2004. The removal of uranium from mining wastewater using algal/microbial biomass. J. Environ. Radioact. 78, 151–177.
Mhadhbi, M., Khitouni, M., Escoda, L., Sunol, J.J., Dammak, M., 2010. Characterization of mechanically alloyed nanocrystalline Fe(Al). J. Nanomat. 2010, 8.
Naeem, A., Westerhoff, P., Mustafa, S., 2007. Vanadium removal by metal (hydr) oxide adsorbents. Water Res. 41, 1596–1602.
Nwe nwe, S., Lwin, T.S., Kay, T.L., 2008. Study on extraction of lanthanum oxide from monazite concentrate. World Acad. Sci. Eng. Technol. 2, 10–20.
Organization, W. H, 2004. Uranium in drinking-water : background document for development of WHO guidelines for drinking-water quality. World Health Organ. 03, 118.
Rein, M., 2013. Technology for the removal of radionuclides from natural water and waste management: state of the art Proceedings of the Estonian Academy of Sciences. Tallin. Chem. Engr 122–132.
Riantong, S., Worasit, T., Teeraporn, K., Chiraporn, S., 2013. Extraction and properties of cellulose from banana peels. J. Sci. Technol. 21, 201–213.
Riodan, C., Bustard, M., Putt, R., Mchale, A.P., 1997. Removal of uranium from solution using residual brewery yeast: combined biosorption and precipitation. Biotechnol. Lett. 19, 385–387.
Sachin, C.G., Sanjeev, R.S., 2014. Equilibrum and kineticss study of uranium(IV) from aqueous solution by citrus limetta peels. J.Radioanal Nucl. Chem. 302, 451–457.
Sheree, B., 2011. South Africa 'not Managing' Impact of Uranium Mining, Says New Report. Saturday-star. IOL, SA.
Spiro, D.A., Xiaoping, Z., Marc, F., Remy, S., 2016. Polymer-supported bifunctional amidoximes for the sorption of uranium from seawater. Ind. Eng. Chem. Res. 55, 4208–4216.
Suryanarayana, C., 2001. Mechanical alloying and milling. Prog. Mater. Sci. 46, 1–184.
Talip, Z., Eral, M., Hiçsonmez, U., 2009. Adsorption of thorium from aqueous solutions by perlite. J. Environ. Radioact. 100, 139–143.
Venkateswarlu, K., Sandhyarani, M., Nellappan, T.A., Rameshababu, N., 2014. Estimation of crystallite size, lattice strain and dislocation density of nanocrystalline carbonate substituted hydroxyapatite by X-ray peak variance analysis. Procedia Mater. Sci. 5, 212–221.
Weijuan, L., Zuyi, T., 2002. Comparative study on Th(IV) sorption on alumina and silica from aqueous solutions. J. Radioanal. Nucl. Chem. 254, 187–192.
Yuehe, L., Chien, M.W., Fred, M.J., Russ, D.B., 1994. Supercritical fluid extraction of thorium and uranium ions from solid and liquid materials with fluorinated @-Diketones and tributyl phosphate. Department of chemistry, University of Idaho, Moscow, Idaho 83843. Environ. Sci. Technol. 28, 1190–1193.